DOI 10.1007/s11204-023-09886-z
Soil Mechanics and Foundation Engineering, Vol. 60, No. 3, July, 2023 (Russian Original No. 3, May-June, 2023)

EXPERIMENTAL INVESTIGATIONS

FATIGUE AND ACOUSTIC EMISSION CHARACTERISTICS OF GRANITE UNDER DIFFERENT CYCLIC LOADING PATHS

UDC 624.131.25:624.131.385

Q. W. Zhang, J. Q. Xiao,* and S. K. Zhang
School of Civil Engineering and Architecture, Anyang Normal University, Anyang, Henan, China,
*Corresponding author E-mail: aynuxjq@126.com.

A large number of experiments were performed to systematically investigate the evolution of the acoustic emission characteristics, dynamic elastic modulus, and axial residual strain of rock under different cyclic loading paths. These results provide experimental support for the damage accumulation and fatigue/failure characteristics of rock structures, and for the construction of a new nonlinear fatigue cumulative damage model suitable for rock materials. More active acoustic emissions are associated with greater acoustic emission intensity, which reflects the association between the dynamic elastic modulus and greater damage. Under increasing cyclic loading, the axial residual strain increases stepwise with increasing load level, following a nonlinear function. Under decreasing cyclic loading, the axial residual strain decreased stepwise and nonlinearly with decreasing load level.

Introduction

Dynamic loads (e.g., earthquakes, blasting, drilling, traffic) are frequently encountered in rock engineering. Cyclic loading is known to often cause sudden rock failure at stress lower than that predicted based on the material compressive strength under monotonic conditions [1]. Fatigue theory tells us that if we want to estimate the residual life of a structure, we must know its damage state, stress state, and load process to calculate the cumulative damage. Loading history strongly influences cumulative damage. It is therefore of great significance to study the development law of rock damage under different cyclic loading paths. A range of research achievements has been made in the study of cyclic loading of rock, such as fatigue deformation [2-7], fatigue damage [7, 8], hysteretic behavior [9], dampening effect [10], and acoustic emission characteristic [11, 12]. Blokhin et al. [3] analyzed the specified effects in geomaterials with different physical and mechanical properties using infrared radiation measurements. Wang et al. [6] studied volume deformation under cyclic loading, and found that the critical stress level value from volume shrinkage to volume swelling can be considered as the threshold of fatigue failure. For granite samples, Xiao et al. [7] discussed the advantages and disadvantages of six kinds of definition methods of the damage variables such as the elastic modulus method, ultrasonic wave velocity method, dissipative energy method, maximal variation method, residual strain method, and acoustic emission accumulation method. Li et al. [8] derived the evolution equation of a power function type with low cycle fatigue damage by applying the cumulative plastic strain to express the damage variable according to damage mechanics theory of continuous media. Chen et al. [10] found that the hysteresis loop of marble and sandstone is a pointed leaf shape; it is therefore believed that increasing viscoelasticity is associated with micro-plasticity within the strain. Both of these affect the lagging modulus and amplitude factors over time. For acoustic emission characteristics, Xiao et al. [11] used fine sandstone and gritstone to conduct uniaxial compression, Brazilian splitting, and variable angular shear experiments, and obtained the acoustic emission counts and energy changes of two rock types under pressure stress, tensile stress, and shear stress. Li et al. [12] investigated the fractal characteristics of the event rate, energy rate, and space distribution of the acoustic emission using three kinds of rock samples under uniaxial cyclic loading and unloading experiments.

Translated from Osnovaniya, Fundamenty i Mekhanika Gruntov, No. 3, May-June, 2023.
0038-0741/23/6003-0229

a  b 

Fig. 1. Granite specimens (a) and rock universal fatigue testing machine (b).

TABLE 1

Loading step	Specimen F09		Specimen F23		Specimen F17		Specimen F20	
	Maximum load, kN	Minimum load, kN	Maximum load, kN	Minimum load, kN	Maximum load, kN	Minimum load, kN	Maximum load, kN	Minimum load, kN
1	186	174	282	78	282	78	90	78
2	210	150	264	96	234	78	138	78
3	234	126	246	114	186	78	186	78
4	246	114	234	126	162	78	210	78
5	258	102	222	138	138	78	234	78
6	264	96	210	150	114	78	246	78
7	270	90	198	162	102	78	258	78
8	276	84	192	168	90	78	270	78
9	282	78	186	174	-	-	282	78

Rock cyclic loading tests can be used to calculate the cumulative damage of rock under a random load, which contributes to the rock fatigue life prediction. The goal of this paper is thus to study the evolution law of the dynamic elastic modulus and the axial residual strain of rock under different loading paths. The results are helpful to further understand the damage accumulation and failure characteristics of rock with a complex load history. The findings provide test support for the construction of a nonlinear fatigue cumulative damage modulus of rock material.

Experimental Conditions and Methodology

The main equipment used in the tests was a RE-8100S rock universal fatigue testing machine (Fig. 1) and a SAEU2S acoustic emission detector. The testing machine is highly integrated and has characteristics including high rigidity, good stability, high automation, and complete functions. The acoustic emission detector well acquires, stores, and analyzes the acoustic emission signals.

Various loads can be exerted on a rock structure in engineering. Four kinds of loading paths were investigated: I) the load level (maximum load and load amplitude) is decreased stepwise while maintaining a constant average cyclic load; II) the load level is increased stepwise while keeping the average cyclic load constant; III) the load level decreased stepwise while maintaining the minimum load constant; and IV) the load level is increased stepwise while keeping the minimum load constant. The loading scheme is as follows. The first stage is static loading at 0.01 mm/s to the average cyclic load. The third stage is still static loading, with the same control mode and loading rate as the first stage, until the rock specimen is damaged. The second stage is multi-step cyclic loading with a loading frequency of 0.5 Hz and a constant cycle number of 100. The specific test parameters in the cyclic loading state are given in Table 1.

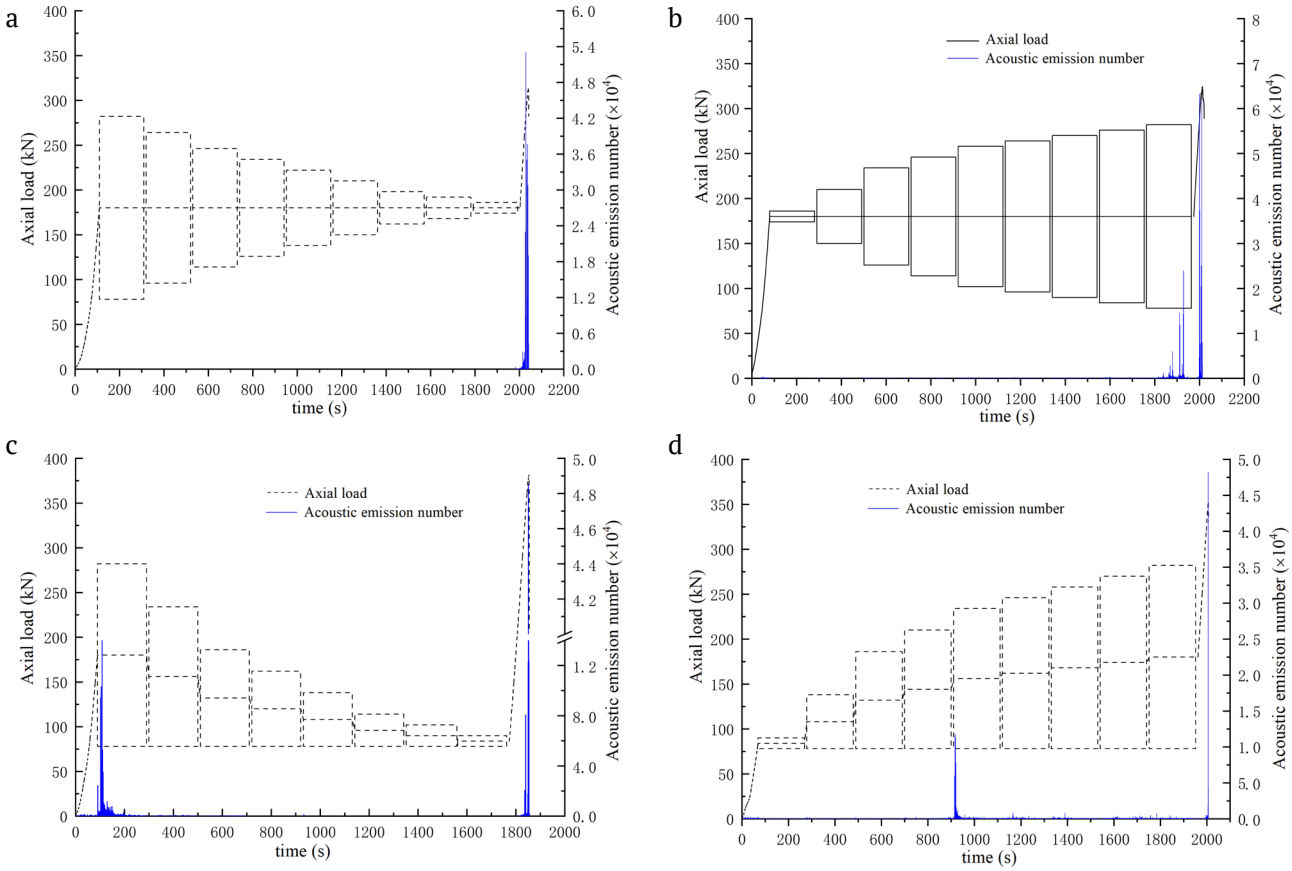

Fig. 2. Acoustic emission number: a) F23, b) F09, c) F17, and d) F20.

Experimental Results and Analysis

The parameters acquired using the SAEU2S detector are the arrival time, amplitude, acoustic emission number, duration, energy, rise count, and rise time. The acoustic emission number rate, energy rate, cumulative acoustic emission number, and cumulative energy can be calculated using a combination of the measured acoustic emission number, energy, and duration. Owing to the similar developing trend between the acoustic emission number and energy, the acoustic emission number is applied in this paper to investigate the acoustic emission characteristics during cyclic loading.

Type I loading path

Figure 2a shows the changes of acoustic emission number of F23. There are few acoustic emission events in the first and second loading stages. During the third stage, strong acoustic activity occurs suddenly when the load exceeds a certain value. For F23, the maximum load of 282 kN in the second stage is similar to the peak load of 313 kN in the third stage. The largest historical load of F23 is therefore relatively high. Although the upper limit stress ratio (i.e., ratio of maximum cyclic load to the peak load under uniaxial compression) is as high as 0.9, few damages are observed.

Figure 3 shows the evolution of the dynamic elastic modulus. The dynamic elastic modulus of F23 increased approximately linearly with decreasing load level. The damage in the cyclic loading stage (Fig. 2a) is minor, and the difference of the dynamic elastic modulus is mainly derived from the different load levels. Higher load levels are associated with denser rock structures and higher elastic performance. On the contrary, lower load levels are associated with looser rock structures and worse elastic performance. The dynamic elastic modulus sharply decreased in the several early cycles. This illustrates that the several previous cycles

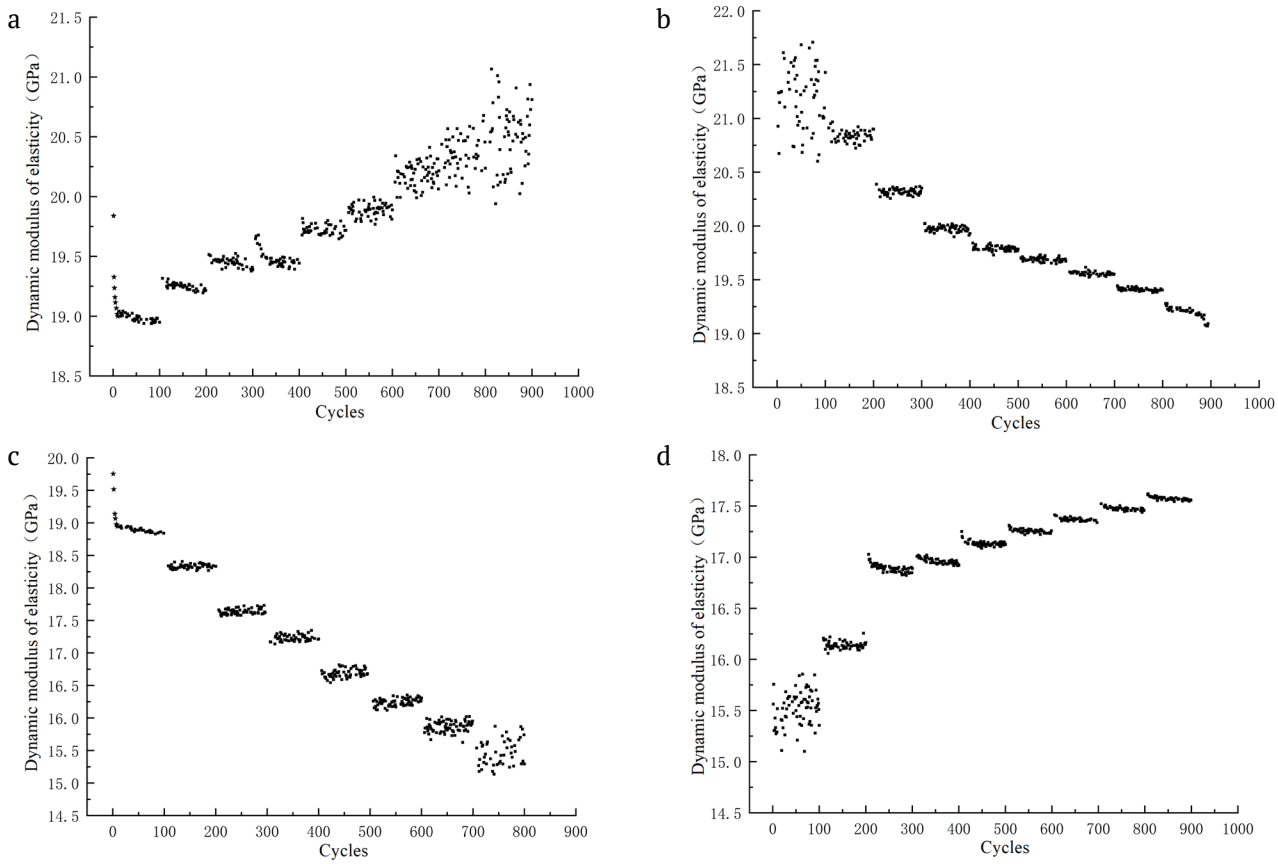

Fig. 3. Dynamic elastic modulus: a) F23, b) F09, c) F17, and d) F20.

had a great influence on the rock structure. Combined with Fig. 2a, the structural adjustment inside the rock specimen led to a drastic decrease rather than damage accumulation. In the first cyclic loading step, except for the previous several cycles, the dynamic elastic modulus in the subsequent loading process slightly decreased, which indicates that only a very small amount of damage had accumulated.

The axial residual strain is illustrated in Fig. 4. The axial residual strain of F23 linearly decreased stepwise with decreasing load level. However, in each cyclic loading step, the axial residual strain was basically maintained. Damage is usually the major factor affecting the axial residual strain during each constant-amplitude cyclic loading step owing to the load level being kept at a constant value. Comparison Fig. 3a, it can be inferred that the axial strain rapidly increased, and increased axial residual strain caused by the increased axial strain was much larger than that of the decreased axial residual strain caused by the reduction of the dynamic elastic modulus.

Type II loading path

Figure 2b demonstrates the change of the acoustic emission number of F09. There are few acoustic emission events during the first static loading stage and the first eight steps of cyclic loading stage. A significant increase can be observed during the ninth cyclic loading step. It can be found that the reason for the sudden increase does not lie in the fact that the maximum cyclic load had exceeded the largest historical load of F09, the sudden increase reflected rapid damage development when the damage has been accumulated to a certain extent. After a short quiet period, the acoustic emission activity increased remarkably when the applied load exceeded the largest historical load, and the specimen was soon thereafter destroyed.

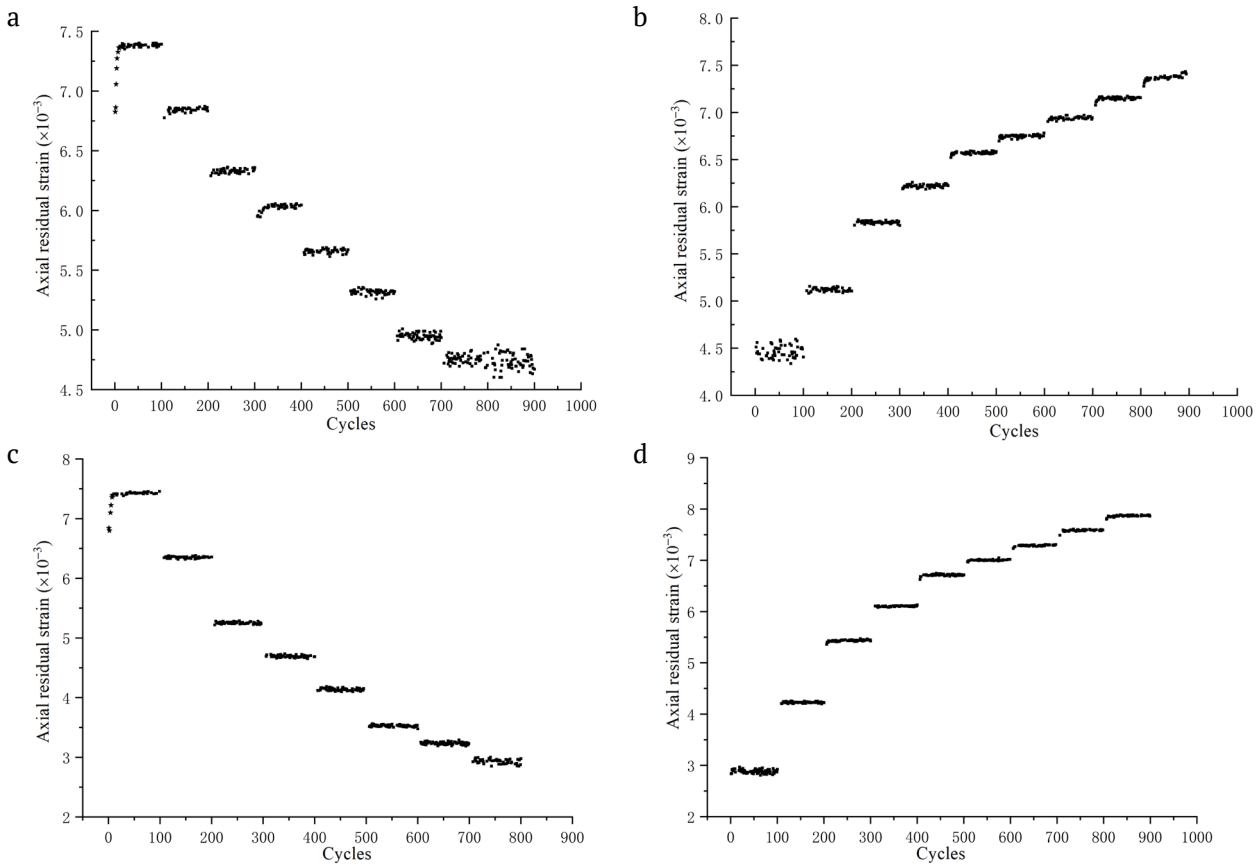

Fig. 4. Axial residual strain: a) F23, b) F09, c) F17, and d) F20.

Figure 3b shows the evolution law of the dynamic elastic modulus of F09. It can be seen that the dynamic elastic modulus decreases stepwise with increasing load level. and the evolution curve is S-shaped, which can be divided into three stages of development. The first stage is from the first cyclic loading step to the fourth cyclic loading step, and the decrease rate of the dynamic elastic modulus with increasing load is relatively higher. The second stage is from the fifth to eighth cyclic loading step, and the decrease rate of the dynamic elastic modulus remains essentially constant with increasing load level stepwise remains with an approximately constant value. The third stage is the ninth cyclic loading step, during which the decrease rate of the dynamic elastic modulus gradually increased because of the rapid development and damage accumulation.

The axial residual strain of F09 increased nonlinearly with increasing load level, and its growth rate gradually decreased (Fig. 4b). The major influencing factors for the axial residual strain are the load level and damage. The influence of the load level is reflected in the gap between steps, while the influence of damage is reflected in the variation of axial residual strain during cyclic loading of the same level. The gap between steps decreases with decreasing influence from the load level, and the variation in the same step increases because of the increasing influence from damage. Combined with Fig. 4a, the axial residual strain development law is opposite when the cyclic loading path is opposite. The axial residual strain decreases linearly when the cyclic load decreases, and increases nonlinearly when the cyclic load increases.

Type III loading path

Figure 2c shows the change of acoustic emission number of F17. There are two notable acoustic emission active periods: one located in the first level of cyclic loading, the second in the second stage of stat-

ic loading. The first sharp increase occurs because the load level surpasses the maximum historical load of the sample. The second sharp increase is when the sample approaches destruction, and micro-cracks further expand and connect.

The dynamic elastic modulus of F17 (Fig. 3c) decreased linearly with decreasing load level. In the first stage of cyclic loading, the dynamic elastic modulus of the first few cycles rapidly decreased and then maintained a decreasing trend at a certain rate. Combined with Fig. 2c, the change of dynamic elastic modulus is closely related to the acoustic emission intensity. The dynamic elastic modulus does not exhibit an obvious variation tendency aside from the first level cyclic loading, and the acoustic emission activity is negligible. This demonstrates that the damage is very small, and the difference of the elastic modulus between the stages is derived from the load level differences.

As shown in Fig. 4c, the axial residual strain of F17 gradually decreased nonlinearly and the gap between stages gradually decreased with decreasing load level. The special case is the first stage, in which the axial residual strain sharply increases in the first few cycles and then remains unchanged. The axial residual strain remains basically unchanged in the other cycle stages.

Type IV loading path

The acoustic emission activity of F20 (Fig. 2d) sharply increased at two moments: the first is the initial stage of the fifth cycle loading, and clearly shows that the load level exceeded the maximum load of history; the second moment is when the destruction occurs, in which crack propagation and penetration produced a strong acoustic emission. The whole process can be divided into two stages. In the previous stage, there were few acoustic emission signals except for the first static loading process. In the latter stage, the intensity of acoustic emission activity is not very large, but the frequency is very high.

Figure 3d shows the development of the dynamic elastic modulus of F20. The dynamic elastic modulus increases nonlinearly with increasing load level. Similar to F09, higher load levels are associated with denser structures and larger dynamic elasticity modulus. In contrast, lower load levels and associated with sparser structures, and smaller dynamic elasticity modulus. Under same level cyclic of loading, the difference between dynamic elastic modulus is substantial when the load level is low, which mainly comes from the change of the sample structure. When the load level becomes higher, the difference is not only related to the rock structure changes but also to the accumulation of damage.

The axial residual strain of F20 (Fig. 4d) increases nonlinearly with increasing load level, and the growth rate gradually decreases. In the process of continuous cyclic loading at all levels, the axial residual strain slightly increases at the beginning of loading, and then remains constant.

Conclusions

1. Generally speaking, in stepwise cyclic loading, higher load levels result in more acoustic emission events. In step-up cyclic loading, acoustic emission events are rare before the load is not greater than the maximum load of history. When the load exceeds the maximum load of history, the Kaser effect is obvious and the number and intensity of the acoustic emission increases sharply. Subsequently, the number and intensity of acoustic emission substantially decreases. During the stepwise reduction of the cyclic loading, if the upper limit load of the first level exceeded the historical maximum load, the acoustic emission activity would be relatively active in levels-1 and -2 cyclic loading, then enter a quiet period until the specimen approaches damage. If the upper limit load of the first stage does not exceed the historical maximum load, the whole cyclic loading phase will be in a quiet period.

2. During stepwise cyclic loading, the evolution of the dynamic elastic modulus is not only related to the damage, but also to the rock internal structural changes. Higher activity acoustic emissions are associated with greater acoustic emission intensities, in which greater damage is associated with smaller dynamic elastic modulus. When the average load is constant, the load level is higher, the dynamic elastic modulus is smaller. Similarly, load levels are associated with a lower dynamic elastic modulus. When the lower limit load is constant, higher load levels are associated with larger dynamic elastic modulus, and lower load levels are associated with smaller dynamic elastic modulus.

3. In the stepwise increasing process of cyclic loading, the axial residual strain increases nonlinearly with increasing load level. In the step-reducing process of cyclic loading, the axial residual strain decreases nonlinearly with increasing load level.

Acknowledgments

The authors gratefully acknowledge the support of this work by the scientific and technological project of Henan Province of China under Grant No. 212102310091.

References

1. A. V. Lavrov and Y. L. Filymonov, *Acoustic Effect of Memory in Rocks*, Publishing House of Moscow State Mining University, Moscow (2004).
2. V. I. Sheinin, D. I. Blokhin, I. B. Maksimovich, and E. P. Sarana, "Experimental research into thermo-mechanical effects at linear and nonlinear deformation stages in rock salt specimens under cyclic loading," *J. Min. Sci.,* **52**(6), 1039-1046 (2016).
3. D. I. Blokhin and V. I. Sheinin, "Thermomechanical effects in different geomaterials in limiting behavior of cyclic loading," *IOP Conf. Series: Earth and Environmental Science,* **773**(1), 012055 (2021).
4. A. S. Voznesenskii, Y. O. Kutkin, M. N. Krasilov, and A. A. Komissarov, "The influence of the stress state type and scale factor on the relationship between the acoustic quality factor and the residual strength of gypsum rocks in fatigue tests," *Int. J. Fatigue,* **84**(3), 53-58 (2016).
5. X. R. Ge, Y. Jiang, Y. D. Lu, and J. X. Ren, "Testing study on fatigue deformation law of rock under cyclic loading," *Chin. J. Rock Mech. Eng.,* **22**(10), 1581-1585 (2003).
6. Z. C. Wang, S. C. Li, L. P. Qiao, and J. G. Zhao, "Fatigue behavior of granite subjected to cyclic loading under triaxial compression condition," *Rock Mech. Rock Eng.,* **46**(6), 1603-1615 (2013).
7. J. Q. Xiao, D. X. Ding, F. L. Jiang, and G. Xu, "Fatigue damage variable and evolution of rock subjected to cyclic loading," *Int. J. Rock Mech. Min.,* **47**(3), 461-468 (2009).
8. S. C. Li, J. Xu, Y. Q. Tao, X. J. Tang, and H. W. Yang, "Low cycle fatigue damage model and damage variable expression of rock," *Rock and Soil Mech.,* **30**(6), 1611-1614 (2009).
9. J. Q. Xiao, D. X. Ding, G. Xu, and F. L. Jiang, "Inverted S-shaped model for nonlinear fatigue damage of rock," *Int. J. Rock Mech. Min.,* **46**(3), 643-648 (2009).
10. Y. P. Chen, and S. J. Wang, "Elastoplastic response of saturated rocks subjected to multilevel cyclic loading," *Rock Soil Mech,,* **31**(4), 1030-1034 (2010).
11. F. K. Xiao, G. Liu, T. Qin, and R. X. Zhao, "Acoustic emission (AE) characteristics of fine sandstone and coarse sandstone fracture process under tension-compression-shear stress," *Chin. J. Rock Mech. Eng.,* **35**(S2), 3458-3472 (2016).
12. S. L. Li, C. Y. Lin, J. X. Mao, Y. R. Huang, and J. Y. Hu, "Experimental study on fractal dimension characteristics of acoustic emission of rock under multilevel uniaxial cyclic loading," *Eng. Mech.,* **32**(9), 92-99 (2015).